MINNEAPOLIS • MAY 20-24, 2018

2018 STLE Annual Meeting & Exhibition

May 20-24, 2018
Minneapolis Convention Center
Minneapolis, Minnesota

Commissioning of a High Speed Rolling-element Bearing Rig: Preliminary Results

TRACK OR CATEGORY
Rolling Element Bearings

Dadouche, Azzedine[1]; Kerrouche, Rami[1,2], Boukraa, Salah[2]

[1] Aerospace Centre, National Research Council Canada, Ottawa, ON, Canada
[2] Institute of Aeronautical and Space Studies, University Saad Dahlab of Blida 1, Blida, Algeria

INTRODUCTION

Rolling element bearings represent critical components in rotating machinery especially aircraft engines and accessory gearboxes. They are required to operate reliably under high temperature and speed conditions well over 3 million DN (bearing bore in millimeter x shaft speed in rpm) where hybrid technology is being investigated by numerous engine manufacturers.
As a result, there has been an enormous amount of work done in the field over the last five decades where different test rigs have been built for that purpose. For instance, Holmes [1] tested ball bearings with a 125 mm bore at speeds up to 24 krpm (3.0 MDN) to determine skidding characteristics. Similarly, in their experimental work, Bamberger et al. [2] studied the effect of speed and load on the performance operation of a 120 mm bore angular contact ball bearing. They found that significant skidding occurred at the highest speed of 25 krpm.
This paper describes the operation of a high-speed bearing rig instrumented with state-of-the-art sensors to study performance characteristics of rolling-element bearings operating at extreme conditions.
A typical aircraft engine roller bearing was used during the commissioning phase of the rig. Preliminary results of the main bearing characteristics under controlled operating conditions are presented.

BEARING TEST RIG

The rolling-element bearing test facility is composed of four main units as depicted in Figure 1:

1. The hydraulic power pack (HPP) unit drives the rig's shaft via a hydraulic motor and pulley/belt mechanism (Figure 2) and allows the control of the load applied radially on the test bearing through a hydralic cylinder. A 30 hp electric motor drives the oil pump of the HPP which provides pressurized oil (up to 34.5 MPa, 5000 PSI) to the hydraulic motor which can reach speeds up to 25,000 rpm. Output torque of the hydraulic motor depends on speed and varies from 7.6 N.m (67 lb.in) at 1000 rpm down to 5.75 N.m (51 lb.in) at 25,000 rpm.
2. The lubrication system allows the supply of oil to the test bearing at the desired oil flow and temperature. The main oil tank is equipped with an electric heater that allows warming up the oil to temperatures up to 120°C (depending on test requirements). An electric motor drives a gear pump to

circulate oil in the lubrication circuit. Oil flows through a heat exchanger, flow meter, oil control valve and finally reaches the test bearing. The heat exchanger allows the control of the oil temperature using a PID controller; whereas, the oil control valve allows the adjustment of the oil flow being fed to the test bearing using either under race or jet lubrication techniques.

3. Radial loads up to 4,450N (1000 lb) can be applied to the test bearing using a hydraulic ram by way of an overhead cable-pulley system (Fig. 2).The loading system is composed of a hydraulic cylinder, spring and pulley-cable system. The cylinder has two ports: the first one allows the application of the load using the pressurized hydraulic oil of the HPP and the second one uses compressed air to keep a back pressure in the cylinder (Fig. 3). The load cell is located between the upper pulley and the spring to record the applied load under testing conditions. The spring contributes in isolating the load cell from vibrations during operation.
4. The rotor/bearing system is depicted in Figure 4. It features an overhung, simply-supported shaft, and is capable of speeds above 35 krpm through a 0.5 : 1 belt and pulley system (Fig. 2). The bearing under test is located at the overhung section of the shaft and can be lubricated via jet or under-race. A telemetry system is used to measure the bearing inner ring temperature (Figs. 2 and 4).

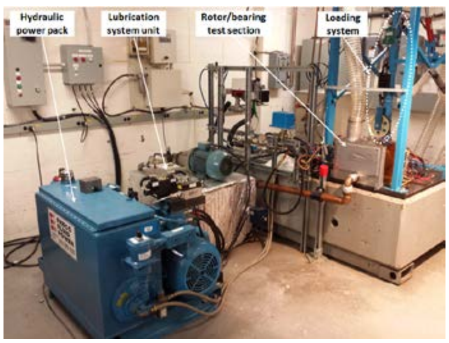

Figure 1. General view of the test facility

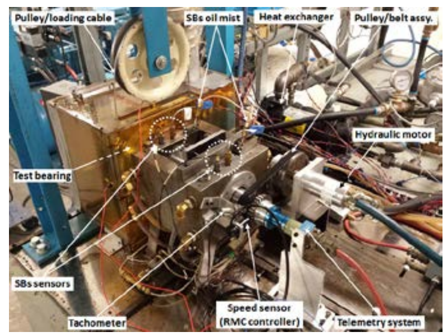

Figure 2. Bearing rig drive system

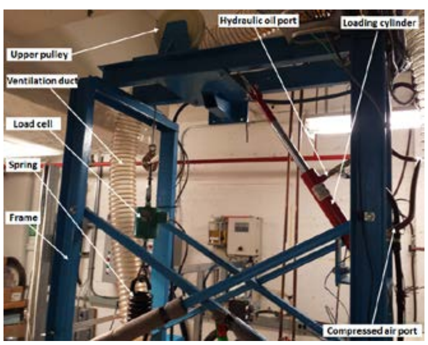

Figure 3. Loading system

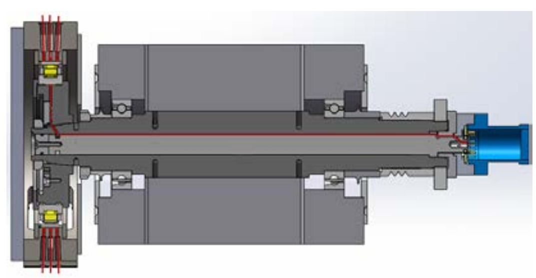

Figure 4. Rotor/bearing system

TEST BEARING & INSTRUMENTATION

In order to facilitate work on the test section and to improve the interface between the test bearing and the test rig, the inner ring of the bearing under test is mounted on a hub, which engages with the shaft by a self-releasing taper. This allows the entire test bearing assembly (hub, bearing, and housing) to be removed from the test rig as a single unit using a custom made puller. This configuration also allows testing bearings with different bores without the need of changing the shaft.

The bearing under test is a 90 mm bore roller bearing with 26 rollers. It is heavily instrumented with thermocouples (Fig. 5a) in addition to three accelerometers to measure vibrations in the vertical, horizontal and axial directions. Shaft speed, bearing radial load and oil flow are also measured during testing. Furthermore, a friction torque mechanism allows the determination of the power loss within the bearing via measurement of the bearing's tangential friction force. Specialized instrumentation also allows the evaluation of roller skidding at different operating conditions.

DATA DISCUSSION

In this paper, only preliminary results are presented. The test bearing was under-race lubricated using BP Turbo Oil 2380 at a temperature of 82°C with a constant oil flow rate of 2.33 l/min (0.615 GPM, 5 PPM). Two oil jets located at the 6 and a12 o'clock positions have been used. Oil was supplied into a chamber machined in the hub and then fed to the bearing through internal radial channels under the effect of the centrifugal force as the shaft starts rotating.

Temperature distribution on the outer ring during ramp up to 5 and 15 krpm at a radial load of 223 N is presented in Figs. 5b and 5c. Temperatures stabilize within about 4 minutes after reaching the set speed for the 5 krpm and about 8 min for the 15 krpm case. In both tests, the maximum temperatures are located in the bearing loaded part in the direction of rotation. For the case of 15 krpm, the maximum temperature is located at the 3 O' position. This is in agreement with previous experimental work found in the literature and is mainly due to the shift of the bearing towards the direction of rotation as the speed increases. It is worth mentioning that hot oil was supplied to the bearing about 15 minutes before the start of the tests. During that time, oil evacuates the hub by gravity and passes through the bottom part of the bearing. This explains the higher temperatures recorded at that location especially at the bottom dead center as shown in Figs. 5b and 5c. As the bearing starts rotating, we notice a temperature drop at these locations and then a smooth increase as one would expect. Fig. 6 shows the effect of load and speed on the bearing average temperature. The load has very little effect compared to the speed. As opposed to the outer ring temperature which evolves exponentially with speed, the inner ring temperature seems to evolve linearly (Fig 6b). More tests need to be carried out to determine accurate trends of the temperatures and other key properties.

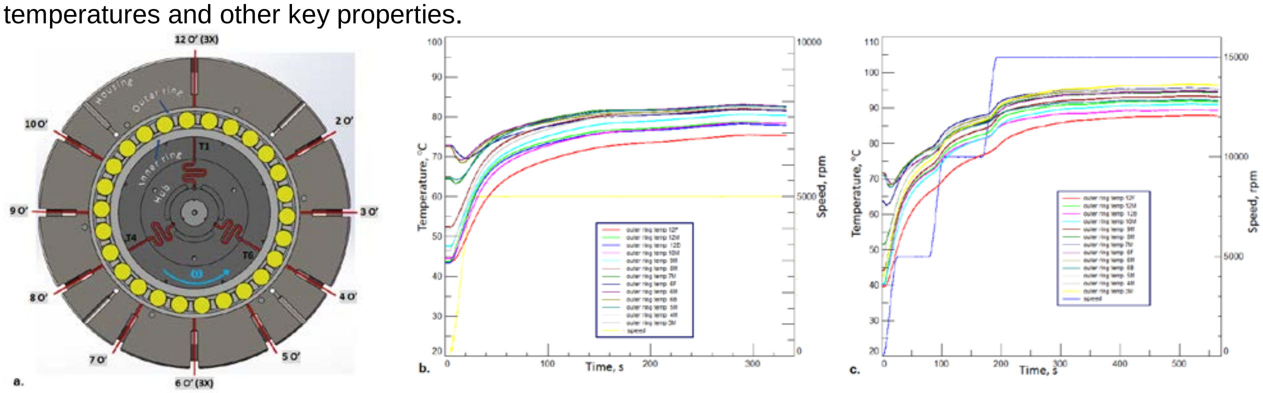

Fig. 5. Bearing temperature: a) thermocouple locations, b) ramp up to 5 krpm, c) ramp up to 15 krpm

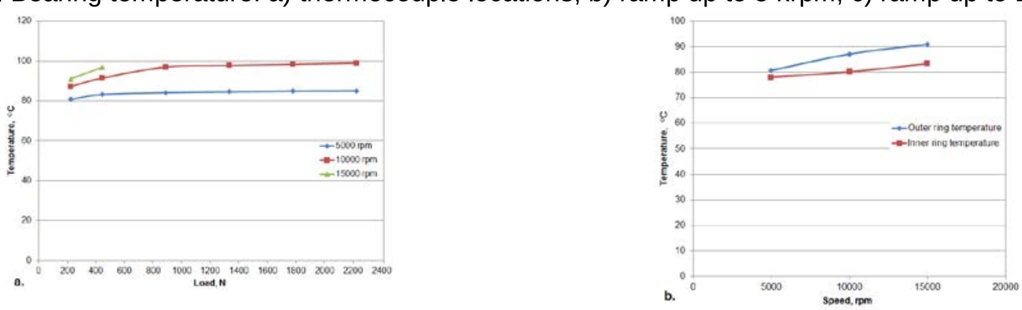

Fig. 6. Effect of load and speed: a) outer ring, b) inner and outer rings at 223N

REFERENCES

[1] Holmes, P.W., 1972, "Evaluation of drilled-ball bearings at DN values to three million: Experimental skid study and endurance tests," NASA technical report No. PWA-4325.

[2] Bamberger, E.N., Zaretsky, E.V. and Signer, 1975, "Effect of speed and load on ultra-high speed ball bearings," NASA technical report No. E-8074.

KEYWORDS

Rolling Bearings:Cylindrical Roller Bearings, Engines:Gas/Jet Turbines, Friction:Hydrodynamic Friction